

# Higgs boson decays and production via gluon fusion at LHC in littlest Higgs models with T-parity

Lei Wang, Jin Min Yang

*Institute of Theoretical Physics, Academia Sinica, Beijing 100190, China*

## Abstract

We study the Higgs boson decays and production via gluon fusion at the LHC as a probe of two typical littlest Higgs models which introduce a top quark partner with different (even and odd) T-parity to cancel the Higgs mass quadratic divergence contributed by the top quark. For each model we consider two different choices for the down-type quark Yukawa couplings. We first examine the branching ratios of the Higgs boson decays and then study the production via gluon fusion followed by the decay into two photons or two weak gauge bosons. We find that the predictions can be quite different for different models or different choices of down-type quark Yukawa couplings and all these predictions can sizably deviate from the SM predictions. So the Higgs boson processes at the LHC can be a sensitive probe for these littlest Higgs models.

PACS numbers: 14.80.Cp,12.60.Fr,11.30.Qc

## I. INTRODUCTION

To solve the fine-tuning problem of the Standard Model (SM), the little Higgs [1] is proposed as a kind of electroweak symmetry breaking mechanism accomplished by a naturally light Higgs sector. The Higgs boson remains light, being protected by the approximate global symmetry and free from one-loop quadratic sensitivity to the cutoff scale. The littlest Higgs model [2] provides an economical approach which implements the idea of the little Higgs. However, due to the tree-level mixing of heavy and light mass eigenstates, the electroweak precision tests can give strong constraints on this model [3], which would require raising the mass scale of the new particles to be much higher than TeV and thus reintroduce the fine-tuning in the Higgs potential [4]. To tackle this problem, a discrete symmetry called T-parity is proposed [5], which forbids those tree-level contributions to the electroweak observables. In the pioneer version of this model (hereafter called model-I) [5], the T-parity is simply implemented by adding the T-parity images for the original top quark interaction to make the Lagrangian T-invariant. A characteristic prediction of this model is a T-even top partner which cancels the Higgs mass quadratic divergence contributed by the top quark.

An alternative implementation of T-parity has recently been proposed (hereafter called model-II) [6], where all new particles including the heavy top partner responsible for cancelling the SM one-loop quadratic divergence are odd under T-parity. An obvious virtue of this model is that the spectrum of the third-generation quark sector is simplified [6].

These littlest Higgs models with T-parity (LHT) mainly alter the property of the Higgs boson and hence the hints of these models can be unravelled from various Higgs boson processes [7, 8, 9, 10, 11]. Since different models have different predictions for Higgs boson processes, it is important to study the models comparatively. In this work we perform such a comparative study for model-I and model-II focusing on the decay branching ratios of the Higgs boson as well as the production at the LHC via gluon fusion followed by the decay into two photons or two weak gauge bosons. Since both models can have two different choices for the down-type quark Yukawa couplings, we will consider the two choices for each model. In our analysis we will show the predictions of these two models and compare with the SM results.

This work is organized as follows. In Sec. II we recapitulate the LHT models with emphasis on model-II since model-I has been intensively discussed in the literature. Then

we perform a comparative study for model-I and model-II focusing on the decay branching ratios of the Higgs boson in Sec. III and the production at the LHC via gluon fusion followed by the decay into two photons or two weak gauge bosons in Sec. IV. Finally, we give our conclusion in Sec. V.

## II. THE LITTLEST HIGGS MODEL WITH T-PARITY

The original littlest Higgs model [2] is based on a non-linear sigma model describing the spontaneous breaking of a global  $SU(5)$  down to a global  $SO(5)$  at an energy scale  $f \sim \mathcal{O}(\text{TeV})$ . The vacuum expectation value of an  $SU(5)$  symmetric tensor  $\Sigma$  is proportional to

$$\Sigma_0 = \begin{pmatrix} 0 & 0 & \mathbb{1} \\ 0 & 1 & 0 \\ \mathbb{1} & 0 & 0 \end{pmatrix}, \quad (1)$$

where  $\mathbb{1}$  represents a unit  $2 \times 2$  matrix. The low energy dynamics of the non-linear sigma model is described in terms of the field

$$\Sigma(x) = e^{i\Pi/f} \Sigma_0 e^{i\Pi^T/f} = e^{2i\Pi/f} \Sigma_0 \quad (2)$$

where

$$\Pi(x) = \sum_{a=1}^{14} \pi^a(x) X^a, \quad (3)$$

with  $\pi^a(x)$  being the Goldstone fields corresponding to 14 broken generators  $X^a$  for the  $SU(5) \rightarrow SO(5)$  breaking.

In the pioneer version of littlest Higgs model with T-parity (model-I), the T-parity in the top quark sector is implemented by simply adding the T-parity images of the original interaction to make the Lagrangian T-invariant. Thus, it predicts a T-even top partner which cancels the Higgs mass quadratic divergence contributed by the top quark. Since there are detailed descriptions for this model in the literature [5, 7], we do not discuss it in detail here. In the following we recapitulate an alternative version of T-parity construction (model-II) [6].

In model-II, to implement T-parity in the fermion sector, it requires the introduction of the mirror fermions. For each SM lepton/quark doublet, under the  $SU(2)_1 \times SU(2)_2$  gauge symmetry, two fermion doublets  $q_1(2, 1)$  and  $q_2(1, 2)$  are introduced. They can be embedded

into the incomplete representation multiplets  $\Psi_1$  and  $\Psi_2$  of  $SU(5)$ . A right-handed  $SO(5)$  multiplets  $\Psi_R$  transforming nonlinearly under the full  $SU(5)$  is introduced to give mass to the extra fermions. The field content can be expressed as

$$\Psi_1 = \begin{pmatrix} q_1 \\ 0 \\ 0 \end{pmatrix}, \quad \Psi_2 = \begin{pmatrix} 0 \\ 0 \\ q_2 \end{pmatrix}, \quad \Psi_R = \begin{pmatrix} \psi_R \\ \chi_R \\ \tilde{\psi}_R \end{pmatrix}, \quad (4)$$

where  $q_A = -\sigma_2(u_{L_A}, d_{L_A})^T = (id_{L_A}, -iu_{L_A})^T$  with  $A = 1, 2$  and  $\tilde{\psi}_R = (id'_R, -iu'_R)^T$ . The second component of  $\psi_R$  is  $-iq_R$ . The mirror fermions can obtain  $\mathcal{O}(f)$  mass via

$$\mathcal{L}_\kappa = -\kappa_{ij} f (\bar{\Psi}_2^i \xi + \bar{\Psi}_1^i \Sigma_0 \xi^\dagger) \Psi_R^j + h.c., \quad (5)$$

where  $\xi = e^{i\Pi/f}$ ,  $\Omega \equiv \text{diag}(1, 1, -1, 1, 1)$ , and  $i, j = 1, 2, 3$  are the generation indices. For simplicity, we assume flavor diagonal and hence we have a universal  $\kappa$  in our study. The fields transform under  $SU(5)$  as

$$\Psi_1 \rightarrow V^* \Psi_1, \quad \Psi_2 \rightarrow V \Psi_2, \quad \Psi_R \rightarrow U \Psi_R, \quad \xi \rightarrow V \xi U^\dagger = U \xi \Sigma_0 V^T \Sigma_0, \quad \Sigma \rightarrow V \Sigma V^T, \quad (6)$$

where  $V$  denotes the  $SU(5)$  rotation, and  $U$  is the unbroken  $SO(5)$  rotation and is a non-linear representation of the  $SU(5)$ . Under T-parity the transformation laws are defined as

$$\Psi_1 \rightarrow -\Omega \Sigma_0 \Psi_2, \quad \Psi_R \rightarrow -\Omega \Psi_R, \quad \xi \rightarrow \Omega \xi^\dagger \Omega, \quad (7)$$

here the transformation of  $\Psi_1$  follows [12], and Eq. (5) has the full  $SU(5)$  global symmetry and thus we have  $q_1 \rightarrow -q_2$  and  $\Sigma \rightarrow \tilde{\Sigma} = \Sigma_0 \Omega \Sigma^\dagger \Omega \Sigma_0$  under T-parity. Under the above transformations, the Lagrangian is T-invariant.

The Lagrangian in Eq. (5) contains the new Higgs boson interactions and the mass terms. For the first and second generations we have

$$\mathcal{L}_\kappa \simeq -\sqrt{2} \kappa f \left[ \bar{d}_{L-} d'_R + \frac{1+c_\xi}{2} \bar{u}_{L-} u'_R - \frac{1-c_\xi}{2} \bar{u}_{L-} q_R + \frac{s_\xi}{\sqrt{2}} \bar{u}_{L+} \chi_R \right] + h.c., \quad (8)$$

where we ignored the generation indices, and  $c_\xi \equiv \cos \frac{v+h}{\sqrt{2}f}$  and  $s_\xi \equiv \sin \frac{v+h}{\sqrt{2}f}$  come from the non-linear sigma model field  $\xi$ , with  $h$  and  $v$  being the neutral Higgs boson field and its vacuum expectation value, respectively. The fermion  $u_{L-} = (u_{L_1} + u_{L_2})/\sqrt{2}$  is T-odd, which together with  $u'_R$  gets a mass, and  $u_{L+} = (u_{L_1} - u_{L_2})/\sqrt{2}$  is T-even and massless. The same definition also applies to the down-type quarks. The fields  $q_R$  and  $\chi_R$  can obtain large Dirac

masses by introducing additional fields, as discussed in [5]. In our study we assume both masses are 3.5 TeV. From Eq. (8) we can see that the first component of the doublet  $\tilde{\psi}_R$  does not appear and the T-odd down-type quarks have no tree-level coupling with the Higgs boson.

For the top quark interaction sector, in order to cancel the quadratic divergence of the Higgs mass induced by the top quark, it requires the introduction of additional singlets  $U_1$  and  $U_2$ . One can write down their interaction Lagrangian as [6]

$$\mathcal{L}_t = -\frac{\lambda}{2\sqrt{2}} f \epsilon_{ijk} \epsilon_{xy} \left[ (\bar{Q}_1)_i \Sigma_{jx} \Sigma_{ky} U_{R_1} - (\bar{Q}_2 \Sigma_0 \Omega)_i \tilde{\Sigma}_{jx} \tilde{\Sigma}_{ky} U_{R_2} \right] + \text{h.c.}, \quad (9)$$

where the indices  $i, j, k$  run from 1 to 3 whereas  $x, y = 4, 5$ , and  $Q_1 = (q_1, U_1, 0_2)^T$  whereas  $Q_2 = (0_2, U_2, q_2)^T$ . Under T-parity these fields transform as  $Q_1 \rightarrow -\Omega \Sigma_0 Q_2$ ,  $U_{R_1} \rightarrow U_{R_2}$ . Therefore, the T-parity eigenstates are defined as  $U_{L_-} = (U_1 - U_2)/\sqrt{2}$  (T-odd) and  $U_{L_+} = (U_1 + U_2)/\sqrt{2}$  (T-even), and the same definition also applies to the right-handed singlet. Eq. (9) will introduce mixing between the light T-even and the heavy T-even fermions, which can be removed by the additional interactions:

$$\mathcal{L}'_t = -\frac{\lambda'}{2\sqrt{2}} f \epsilon_{lmn} \epsilon_{rs} \left[ (\bar{Q}_2)_l \Sigma'_{mr} \Sigma'_{ns} U_{R_1} - (\bar{Q}_1 \Omega \Sigma_0)_l \tilde{\Sigma}'_{mr} \tilde{\Sigma}'_{ns} U_{R_2} \right] + \text{h.c.}, \quad (10)$$

where  $\Sigma' = \Omega \Sigma^\dagger \Omega$ ,  $\Sigma' \rightarrow \tilde{\Sigma}' = \Sigma_0 \Sigma \Sigma_0$  under T-parity, and the indices  $l, m, n$  run from 3 to 5 whereas  $r, s=1,2$ . Adding  $\mathcal{L}'_t$  to  $\mathcal{L}_t$  and taking  $\lambda' = \lambda$ , we can get the following simple expression for the top quark Yukawa coupling sector

$$\mathcal{L}_t - \mathcal{L}'_t \simeq -\lambda f \left( s_\Sigma \bar{u}_{L_+} U_{R_+} + \frac{1 + c_\Sigma}{\sqrt{2}} \bar{U}_{L_-} U_{R_-} \right) + \text{h.c.}, \quad (11)$$

where  $c_\Sigma \equiv \cos \frac{\sqrt{2}(v+h)}{f}$  and  $s_\Sigma \equiv \sin \frac{\sqrt{2}(v+h)}{f}$  arise from the non-linear sigma model field  $\Sigma$ . The field  $U_{L_+}$  together with  $\chi_R$  gets a Dirac mass in Eq. (5). From Eq.(5) we can get the Higgs boson interactions and the mass terms for the third generation fermions

$$\begin{aligned} \mathcal{L}_\kappa \simeq & -\sqrt{2} \kappa f \left[ \bar{d}_{L_-} d'_{R_+} + \frac{1 + c_\xi}{2} \bar{u}_{L_-} u'_{R_+} - \frac{1 - c_\xi}{2} \bar{u}_{L_-} q_R \right. \\ & \left. - \frac{s_\xi}{\sqrt{2}} \bar{U}_{L_-} q_R - \frac{s_\xi}{\sqrt{2}} \bar{U}_{L_-} u'_{R_+} + \frac{s_\xi}{\sqrt{2}} \bar{u}_{L_+} \chi_R + c_\xi \bar{U}_{L_+} \chi_R \right] + \text{h.c.} \end{aligned} \quad (12)$$

The Yukawa couplings of up-type quarks for the first and second generations are given by a similar Lagrangian as for the top quark, but without introducing any extra singlet fields:

$$\mathcal{L}_u = -\frac{\lambda_u}{2\sqrt{2}} f \epsilon_{ijk} \epsilon_{xy} \left[ (\bar{\Psi}_1)_i \Sigma_{jx} \Sigma_{ky} - (\bar{\Psi}_2 \Sigma_0 \Omega)_i \tilde{\Sigma}_{jx} \tilde{\Sigma}_{ky} \right] u_R + \text{h.c.}, \quad (13)$$

where  $u_R \rightarrow u_R$  under T-parity. Eq.(13) contains the following Higgs boson interactions as well as the mass term for up-type quarks of the first and second generations

$$\mathcal{L}_u \simeq -\frac{\lambda_u}{\sqrt{2}} f_{S\Sigma} u_{L+} u_R + \text{h.c.} \quad (14)$$

After diagonalizing the mass matrix in Eqs.(8,11,12,14), we can get the mass eigenstates and the Higgs couplings. For each SM fermion doublet, there are  $d_-, u_-, q$  (T-odd) and  $\chi$  (T-even). Besides, the top quark has a T-odd partner  $T_-$  which cancels the one loop quadratic divergence of Higgs mass induced by the top quark.

Higgs boson has the couplings with other particles including down-type quarks, leptons, SM gauge bosons, extra gauge bosons and scalar particles. These couplings are same as in model-I and can be found in [7, 13]. Here we list the Higgs boson couplings with the down-type quarks and the SM gauge bosons, normalized with the corresponding couplings in the SM,

$$\begin{aligned} \frac{g_{h\bar{d}d}}{g_{h\bar{d}d}^{\text{SM}}} &\approx 1 - \frac{1}{4} \frac{v_{SM}^2}{f^2} + \frac{7}{32} \frac{v_{SM}^4}{f^4} \quad \text{for Case A,} \\ &\approx 1 - \frac{5}{4} \frac{v_{SM}^2}{f^2} - \frac{17}{32} \frac{v_{SM}^4}{f^4} \quad \text{for Case B,} \\ \frac{g_{hVV}}{g_{hVV}^{\text{SM}}} &\approx 1 - \frac{1}{4} \frac{v_{SM}^2}{f^2} - \frac{1}{32} \frac{v_{SM}^4}{f^4}, \quad (V = Z, W), \end{aligned} \quad (15)$$

where  $G_F = 1/(\sqrt{2}v_{sm}^2)$  with  $v_{sm} = f\sqrt{1 - \cos(\sqrt{2}v/f)}$ . The relation of down-type quark couplings also applies to the lepton couplings.

### III. HIGGS DECAY BRANCHING RATIOS IN LHT MODELS

In both model-I and model-II, the heavy photon  $A_H$  is the lightest T-odd particle with a mass given by

$$M_{A_H}^2 = \frac{g'^2 f^2}{5} - \frac{g'^2 v_{SM}^2}{4}. \quad (16)$$

As discussed in [14], the scale  $f$  in model-I may be as low as 500 GeV, and the constraint in model-II is expected to be even weaker [6]. For  $f = 500$  GeV,  $A_H$  has a mass of about 65 GeV. Therefore, in addition to the SM decay channels, the new decay  $h \rightarrow A_H A_H$  will open for  $m_h \geq 2m_{A_H}$  and the partial width is given by

$$\Gamma(h \rightarrow A_H A_H) = \frac{g_{hA_H A_H}^2 m_h^3}{128\pi m_{A_H}^4} \sqrt{1 - \beta_{A_H}} \left( 1 - \beta_{A_H} + \frac{3}{4} \beta_{A_H}^2 \right), \quad (17)$$

where  $\beta_{A_H} = 4m_{A_H}^2/m_h^2$ . Because  $A_H$  is stable, there are no off-shell decays  $h \rightarrow A_H^* A_H^*$  or  $h \rightarrow A_H A_H^*$ . In the LHT models the partial widths of the Higgs decays to the SM particles can be obtained as  $\Gamma(h \rightarrow XX) = \Gamma(h \rightarrow XX)_{SM} (g_{hXX}/g_{hXX}^{SM})^2$  ( $X$  denotes a SM particle), where  $g_{hXX}/g_{hXX}^{SM}$  is predicted by the LHT models and  $\Gamma(h \rightarrow XX)_{SM}$  is calculated with the code Hdecay [15] (the relevant higher order QCD and electroweak corrections are considered in this code).

Note that in the LHT models the corrections to the tree-level decays  $h \rightarrow f\bar{f}, WW, ZZ$  are mainly from the suppression of the corresponding couplings. For the loop-induced decay  $h \rightarrow gg$ , in addition to the top quark loops, the loops of new T-even and T-odd quarks also come into play. For the decay  $h \rightarrow Z\gamma$ , the  $W$  boson loop contribution is dominant [16] and thus we only consider the alteration of the Higgs coupling with the  $W$  boson. The decay channel  $h \rightarrow \gamma\gamma$  is a focus of our discussion. In addition to the contributions of top quark and  $W$  boson, the new charged heavy fermions, gauge bosons and scalar particles will contribute to the decay  $h \rightarrow \gamma\gamma$ . Following the approach in [17], we calculate the partial decay width of  $h \rightarrow \gamma\gamma$  at one-loop. Because the QCD radiative corrections are rather small [15], our result is precise enough.

In our calculation we take  $\kappa = 1$  and  $\lambda' = \lambda$  in model-II, and  $r = 1$  in model-I. Our calculations show that the results are not so sensitive to these parameters, but very sensitive to the Higgs mass  $m_h$  and breaking scale  $f$ . We take  $100 \text{ GeV} \leq m_h \leq 500 \text{ GeV}$  and  $500 \text{ GeV} \leq f \leq 2 \text{ TeV}$ .

In Fig. 1 we plot the Higgs decay branching ratios versus the Higgs boson mass in model-I and model-II. Comparing the left panels with the right panels, we see that the two models predict very different branching ratios for  $h \rightarrow gg$ . Further, comparing the upper panels with the lower panels, we see that for each model the two cases give quite different branching ratios for  $h \rightarrow gg$  or  $h \rightarrow \gamma\gamma$ . In both models with  $f = 500 \text{ GeV}$ , the new decay  $h \rightarrow A_H A_H$  opens up for  $m_h \geq 130 \text{ GeV}$ . This decay mode can be dominant and over 70% for  $130 \text{ GeV} < m_h < 150 \text{ GeV}$ , then it decreases as  $m_h$  gets large and become comparable with  $h \rightarrow WW^*$  at  $m_h \simeq 160 \text{ GeV}$ . The reason is that the Higgs coupling with  $A_H$  is of the electroweak strength and much larger than the Yukawa coupling of  $b$  quark. For  $130 \text{ GeV} < m_h < 150 \text{ GeV}$ , the decay width of  $h \rightarrow A_H A_H$  is much larger than the decay  $h \rightarrow bb$  and the off-shell decay  $h \rightarrow WW^*$ . Here we fixed  $f = 500 \text{ GeV}$  and did not show the dependence on  $f$ . As  $f$  gets larger, the decay  $h \rightarrow A_H A_H$  becomes less important.

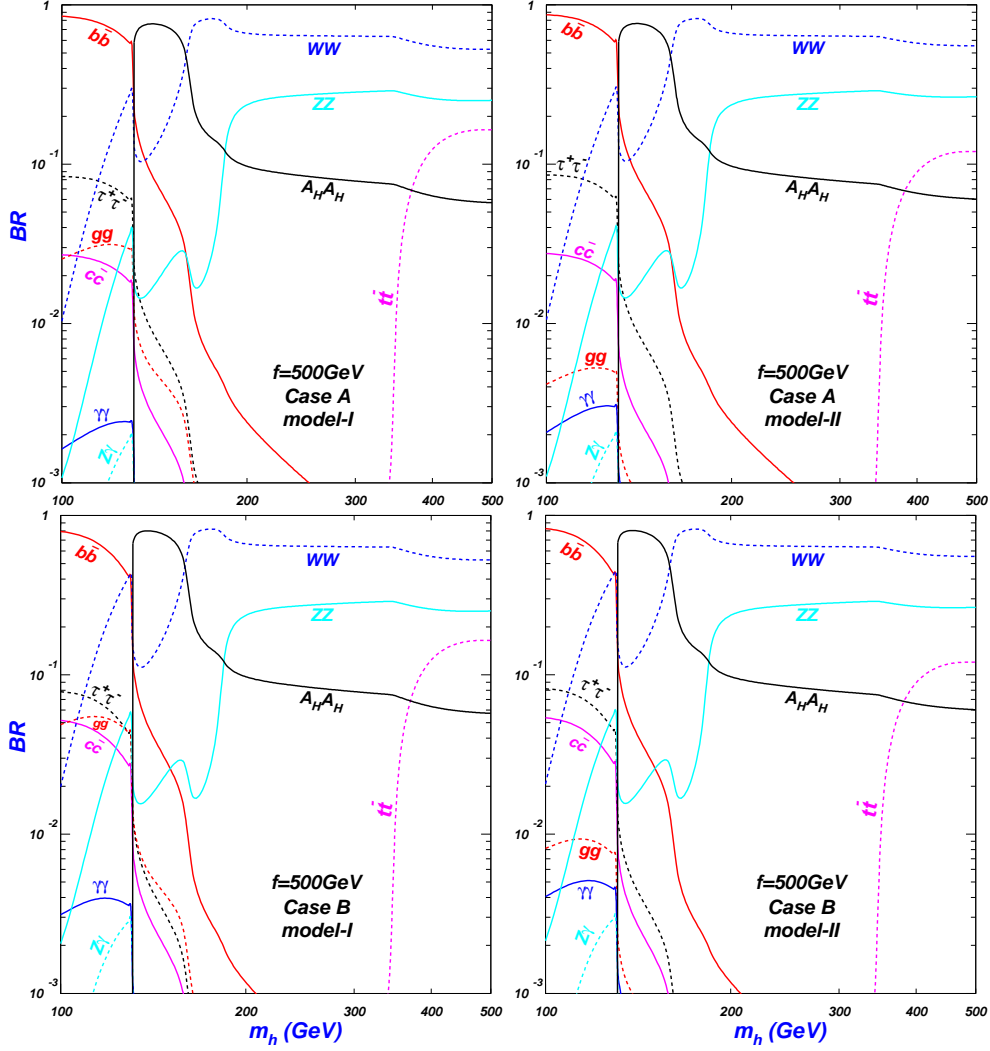


FIG. 1: The Higgs decay branching ratios versus the Higgs mass in model-I and model-II.

In Figs. 2 and 3, we plot the Higgs decay branching ratios normalized to the SM predictions in model-I and model-II for Case A and Case B, respectively. We see that for a small value of  $f$  the two models can predict quite different branching ratios from the SM predictions. As  $f$  gets large, the deviation from the SM prediction for each decay mode becomes small and finally reduce to the SM results when  $f$  is up to 2 TeV. The deviation from the SM prediction is also sensitive to the Higgs boson mass. Again, the results show that the two models predict quite different branching ratios for  $h \rightarrow gg$  or  $h \rightarrow \gamma\gamma$ ; while for other decay modes the two models give the similar results. Besides, the predictions of various branching ratios in Case A and Case B can be sizably different for  $m_h = 120\text{GeV}$  and a small value of  $f$ . In the following we give some explanations for the above features:

- (1) First we explain why the branching ratio of  $h \rightarrow gg$  ( $h \rightarrow \gamma\gamma$ ) in model-II is smaller



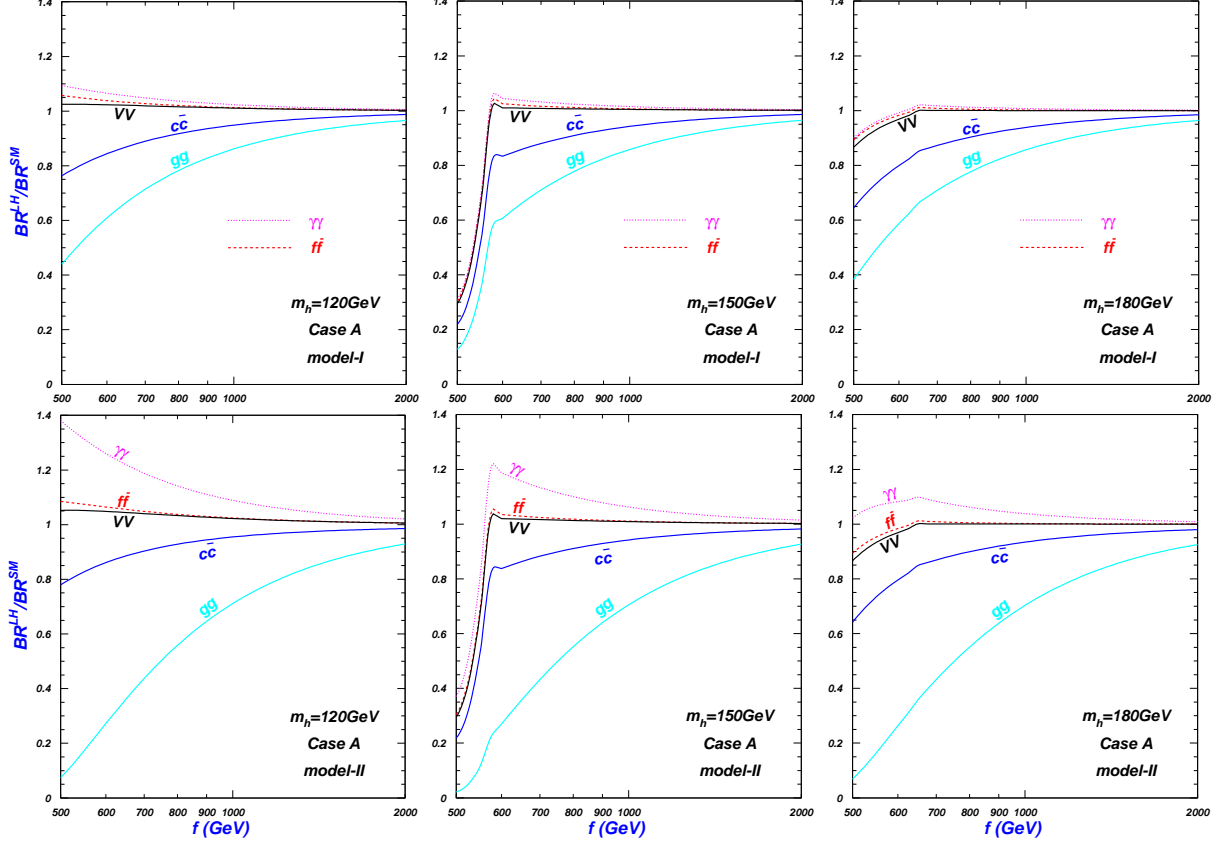


FIG. 2: The Higgs decay branching ratios normalized to the SM predictions in model-I and model-II. For the decay channel  $VV$ ,  $V$  can be  $Z$  or  $W$ , while for  $f\bar{f}$ ,  $f$  denotes a down-type quark or lepton.

(larger) than in model-I. The main contributions of model-I and model-II to the decay  $h \rightarrow gg$  are from the loops of the fermions whose couplings to  $h$  are given by

$$-\frac{m_t}{v}y_t\bar{t}th - \frac{m_T}{v}y_T\bar{T}Th + \sum_{i=1}^3 -\frac{m_{u_i}}{v}y_{u_i}\bar{u}_i u_i h - \frac{m_{q_i}}{v}y_{q_i}\bar{q}_i q_i h - \frac{m_{\chi_i}}{v}y_{\chi_i}\bar{\chi}_i \chi_i h \quad (18)$$

in model-I and

$$-\frac{m_t}{v}y'_t\bar{t}th - \frac{m_{U_-}}{v}y'_{U_-}\bar{U}_- U_- h + \sum_{i=1}^3 -\frac{m_{u_i}}{v}y'_{u_i}\bar{u}_i u_i h - \frac{m_{q_i}}{v}y'_{q_i}\bar{q}_i q_i h - \frac{m_{\chi_i}}{v}y'_{\chi_i}\bar{\chi}_i \chi_i h \quad (19)$$

in model-II. Here all the particles are the mass eigenstates (the diagonalization of the mass matrix was performed numerically in our analysis). The contributions of these fermion loops are not sensitive to the mass values when the fermion masses are much larger than half of the Higgs boson mass. Hence, the contributions of model-I and model-II are approximately proportional to  $y_I^2/v^2$  and  $y'_{II^2}/v^2$ , where  $y_I$  and  $y'_{II}$  denote the sum of  $y$  and  $y'$  in Eqs. (18) and (19), respectively. As  $y'_{II^2}$  is smaller than  $y_I^2$  in

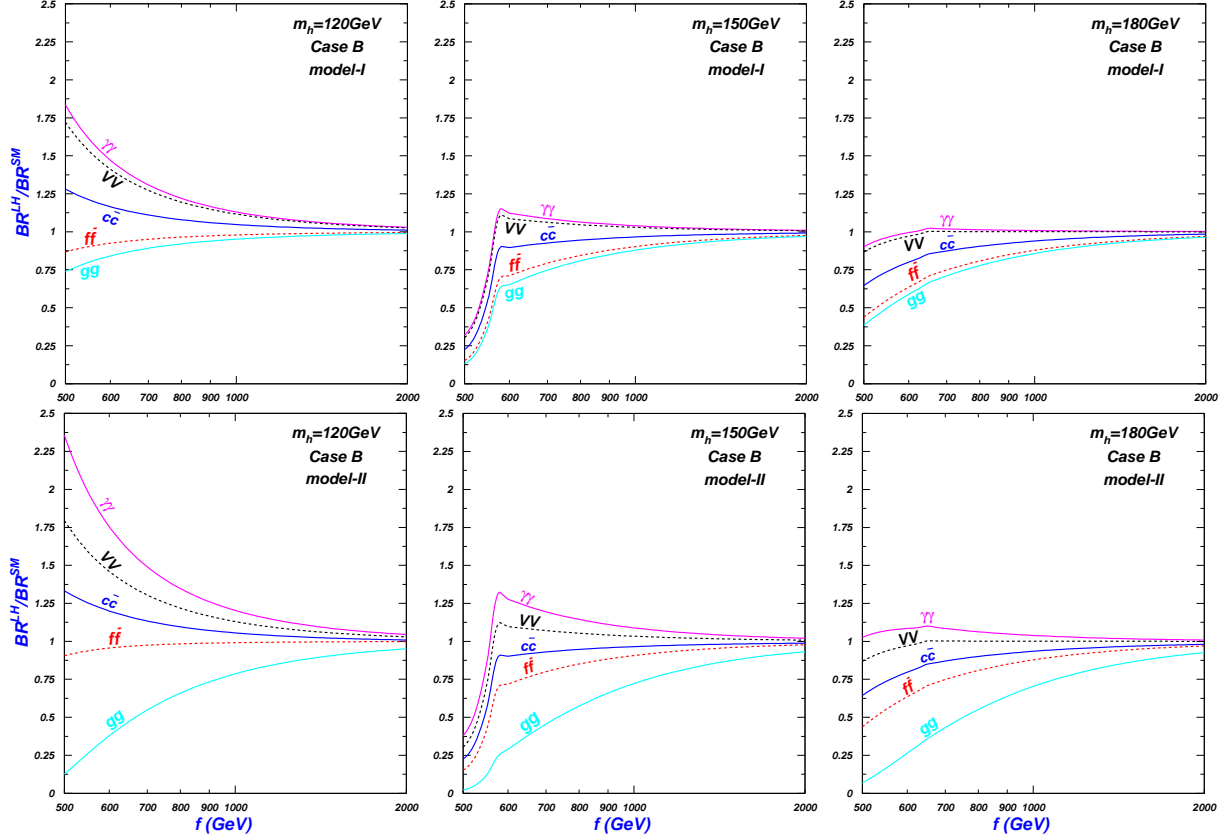


FIG. 3: Same as Fig.2, but for Case B.

the parameter space we chose (for example, Table 1 shows the values of  $y_I$  and  $y_{II}$  for  $f = 700$  GeV), the decay width of  $h \rightarrow gg$  in model-II is thus smaller than in model-I. For the decay  $h \rightarrow \gamma\gamma$ , besides the fermion loops, the boson loops also contribute but with an opposite sign. While the fermion loop contribution in model-II is smaller than in model-I, the contributions of boson loops are equal in both models. The extent of cancellation between fermion and boson loops in model-I is more severe than in model-II. Thus, the decay width of  $h \rightarrow \gamma\gamma$  in model-II is larger than in model-I. On the other hand, for the total decay width of the Higgs boson, depending on the value of the Higgs boson mass, it can be dominated by the decay  $h \rightarrow b\bar{b}$ ,  $h \rightarrow VV$  or  $h \rightarrow A_H A_H$ , and each of these decays has the same width in both models. Therefore, the branching ratio of  $h \rightarrow gg$  ( $h \rightarrow \gamma\gamma$ ) in model-II is smaller (larger) than that in model-I.

- (2) The reason why the two models give similar results for the decay modes of  $c\bar{c}$  and  $f\bar{f}$  ( $f$  is a down-type quark or lepton) is that the two models give respectively the same

TABLE I: The values of  $y$  and  $y'$  in Eqs. (18) and (19) for  $f = 700$  GeV.

$y_t$	$y_T$	$y_{u_1^-} + y_{u_2^-} + y_{u_3^-}$	$y_{q_1^-} + y_{q_2^-} + y_{q_3^-}$	$y_{\chi_1^-} + y_{\chi_2^-} + y_{\chi_3^-}$	$y_I$
0.947	-0.036	-0.104	0.008	0	0.815
$y'_t$	$y'_{U^-}$	$y'_{u_1^-} + y'_{u_2^-} + y'_{u_3^-}$	$y'_{q_1^-} + y'_{q_2^-} + y'_{q_3^-}$	$y'_{\chi_1^-} + y'_{\chi_2^-} + y'_{\chi_3^-}$	$y_{II}$
0.876	-0.169	-0.057	0.001	-0.026	0.625

prediction for the Higgs Yukawa couplings with down-type quarks, leptons, and almost the same prediction for up-type quarks except top quark. Therefore, the branching ratios of these decay channels are similar in both models.

- (3) The  $hb\bar{b}$  coupling in Case B is more suppressed than in Case A, as shown in Eq. (15). For  $m_h = 120$  GeV, the decay  $h \rightarrow b\bar{b}$  is dominant and the total decay width in Case B is much smaller than in Case A. Therefore, the predictions of various branching ratios in Case B can be sizably different from those in Case A for  $m_h = 120$  GeV and a small value of  $f$ .

#### IV. THE RATE $\sigma(gg \rightarrow h) \times BR(h \rightarrow \gamma\gamma \text{ or } VV)$ AT LHC IN LHT MODELS

In the SM the Higgs productions at the LHC are dominated by gluon fusion process. The  $h \rightarrow \gamma\gamma$  channel shows very good sensitivity in the range  $114 \text{ GeV} < m_h < 140 \text{ GeV}$ . For  $2m_W < m_h < 2m_Z$ , the decay  $h \rightarrow WW \rightarrow l\nu l\nu$  provides the most sensitive search channel. For  $m_H > 130 \text{ GeV}$  (except the interval between  $2m_W$  and  $2m_Z$ ), the channel  $h \rightarrow ZZ^* \rightarrow 4l$  provides excellent sensitivity [18]. Especially, for the channel  $h \rightarrow \gamma\gamma$ , with an integrated luminosity  $100 \text{ fb}^{-1}$  ( $10 \text{ fb}^{-1}$ ) from both ATLAS and CMS, the rate  $\sigma(gg \rightarrow h) \times BR(h \rightarrow \gamma\gamma)$  can be measured to 10% (30%) [8, 19]. Once we find a light Higgs boson at the LHC, this channel can provide a test for different models. In the LHT models,  $\sigma(gg \rightarrow h)$  is strongly correlated with  $\Gamma(h \rightarrow gg)$ , which depend on the same effective coupling  $hgg$ . In our results we use  $\sigma(gg \rightarrow h)$  to denote the hadronic cross section of the Higgs production proceeding through  $gg \rightarrow h$  at parton level. We use CTEQ6L [20] for parton distributions, with the renormalization scale  $\mu_R$  and factorization scale  $\mu_F$  chosen to be  $\mu_R = \mu_F = m_h$ .

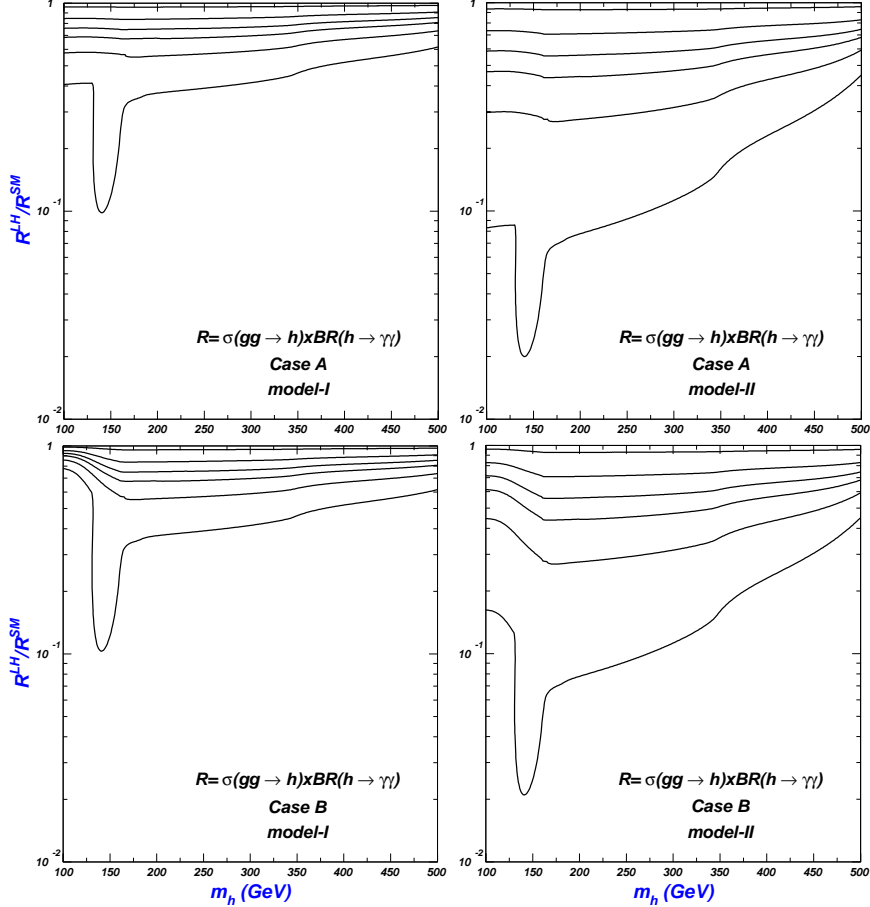


FIG. 4: The value of  $\sigma(gg \rightarrow h) \times BR(h \rightarrow \gamma\gamma)$  normalized to the SM prediction in model-I and model-II. The curves from bottom to top correspond to  $f = 500$  GeV, 600 GeV, 700 GeV, 800 GeV, 1 TeV, 2 TeV, respectively. The cross section  $\sigma(gg \rightarrow h)$  denotes the hadronic cross section proceeding through  $gg \rightarrow h$ .

In Figs. 4 and 5 we plot respectively the rates of  $\sigma(gg \rightarrow h) \times BR(h \rightarrow \gamma\gamma)$  and  $\sigma(gg \rightarrow h) \times BR(h \rightarrow VV)$  ( $V = Z, W$ ) normalized to the SM predictions in model-I and model-II. We see that compared with the SM predictions the LHT models can suppress the rates sizably for a small value of  $f$ . As  $f$  gets large, the suppression is weakened and finally the results reduce to the SM predictions for a sufficiently large  $f$  (about 2 TeV). Further, the two models can give very different predictions. For example, for  $m_h = 150$  GeV and  $f = 500$  GeV, the rates are suppressed to  $10^{-1}$  ( $10^{-2}$ ) relative to the SM predictions in model-I (model-II). The deviation of the predictions between the two models can be understood as follows. The production cross section of  $gg \rightarrow h$  is much smaller in model-II than in model-I since the process  $gg \rightarrow h$  is strongly correlated with the decay  $h \rightarrow gg$  (the decay width of  $h \rightarrow gg$  in model-II is much smaller than in model-I, as shown and explained in the

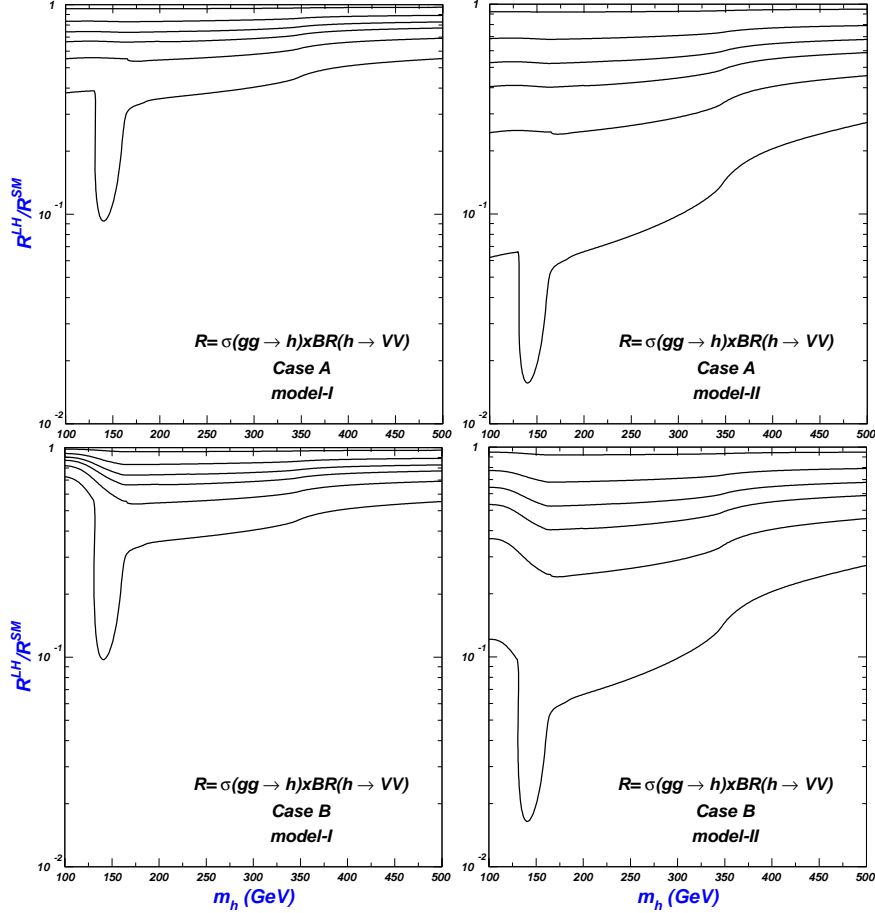


FIG. 5: Same as Fig. 4, but for  $\sigma(gg \rightarrow h) \times Br(h \rightarrow VV)$  ( $V = Z, W$ ).

preceding section). Although the decay branching ratio of  $h \rightarrow \gamma\gamma$  is larger in model-II, the suppression of the production cross section of  $gg \rightarrow h$  is dominant and thus the rate  $\sigma(gg \rightarrow h) \times BR(h \rightarrow \gamma\gamma)$  is smaller in model-II. Besides, Figs. 4 and 5 showed that the predictions in Case A and Case B can be sizably different in the range of  $100 \text{ GeV} \leq m_h \leq 130 \text{ GeV}$  for a small value of  $f$ . The reason is that the two cases give quite different branching ratios for  $h \rightarrow \gamma\gamma$  or  $h \rightarrow gg$  (and thus give different cross sections for  $gg \rightarrow h$ ), as shown and explained in the preceding section.

## V. CONCLUSION

In two typical littlest Higgs models which introduce a top quark partner with different (even and odd) T-parity to cancel the Higgs mass quadratic divergence contributed by the top quark, we calculated the branching ratios of the Higgs boson decays and examined the production at the LHC via gluon fusion followed by the decay into two photons or two weak

gauge bosons. For each model we considered two different choices for the down-type quark Yukawa couplings. From our numerical results we obtained the following observations: (i) For the Higgs decays, we found that with  $130 \text{ GeV} < m_h < 150 \text{ GeV}$  and  $f \simeq 500 \text{ GeV}$ , the new decay  $h \rightarrow A_H A_H$  can be the dominant mode. The two models can give very different branching ratios from the SM predictions. Further, the predictions between the two models can be quite different for  $BR(h \rightarrow \gamma\gamma)$  and  $BR(h \rightarrow gg)$ ; while for other decay modes both models give the similar predictions; (ii) For the rates  $\sigma(gg \rightarrow h) \times BR(h \rightarrow \gamma\gamma)$  and  $\sigma(gg \rightarrow h) \times BR(h \rightarrow VV)$  ( $V = Z, W$ ) at the LHC, both models can give severe suppression relative to the SM predictions, and the predictions of the two models can also differ significantly; (iii) For each model the two different choices for the down-type quark Yukawa couplings can also lead to different results. Therefore, these Higgs processes at the LHC may be a sensitive probe for the little Higgs theory and may even provide a way to distinguish the different models or different scenarios.

### Acknowledgement

We thank C.-P. Yuan for discussions. This work was supported by the National Natural Science Foundation of China (NNSFC) under Nos. 10821504, 10725526 and 10635030.

- 
- [1] N. Arkani-Hamed, A. G. Cohen, H. Georgi, Phys. Lett. B **513**, 232 (2001); N. Arkani-Hamed, A. G. Cohen, T. Gregoire, J. G. Wacker, JHEP **0208**, 020 (2002); N. Arkani-Hamed, *et al.*, JHEP **0208**, 021 (2002); I. Low, W. Skiba, D. Smith, Phys. Rev. D **66**, 072001 (2002); D. E. Kaplan, M. Schmaltz, JHEP **0310**, 039 (2003).
- [2] N. Arkani-Hamed, A. G. Cohen, E. Katz, A. E. Nelson, JHEP **0207**, 034 (2002); S. Chang, JHEP **0312**, 057 (2003); T. Han, H. E. Logan, B. McElrath, L. T. Wang, Phys. Rev. D **67**, 095004 (2003); M. Schmaltz, D. Tucker-smith, Ann. Rev. Nucl. Part. Sci. **55**, 229 (2005).
- [3] C. Csaki, J. Hubisz, G. D. Kribs, P. Meade, J. Terning, Phys. Rev. D **67**, 115002 (2003); J. L. Hewett, F. J. Petriello, T. G. Rizzo, JHEP **0310**, 062 (2003); C. Csaki, J. Hubisz, G. D. Kribs, P. Meade, J. Terning, Phys. Rev. D **68**, 035009 (2003); M. C. Chen, S. Dawson, Phys. Rev. D **70**, 015003 (2004); M. C. Chen *et al.*, Mod. Phys. Lett. A **21**, 621 (2006); W. Kilian,

- J. Reuter, Phys. Rev. D **70**, 015004 (2004).
- [4] G. Marandella, C. Schappacher and A. Strumia, Phys. Rev. D **72**, 035041 (2005).
- [5] H. C. Cheng and I. Low, JHEP **0309**, 051 (2003); JHEP **0408**, 061 (2004); I. Low, JHEP **0410**, 067 (2004); J. Hubisz, P. Meade, Phys. Rev. D **71**, 035016 (2005).
- [6] H. C. Cheng, I. Low and L. T. Wang, Phys. Rev. D **74**, 055001 (2006).
- [7] C. R. Chen, K. Tobe, C. P. Yuan, Phys. Lett. B **640**, 263 (2006).
- [8] K. Hsieh, C. P. Yuan, Phys. Rev. D **78**, 053006 (2008).
- [9] C. O. Dib, R. Rosenfeld, A. Zerwekh, JHEP **0605**, 074 (2006); L. Wang *et al.*, Phys. Rev. D **76**, 017702 (2007); Phys. Rev. D **75**, 074006 (2007); Phys. Rev. D **77**, 015020 (2008).
- [10] X.F. Han, L. Wang, J. M. Yang, Phys. Rev. D **78**, 075017 (2008).
- [11] R. S. Hundi, B. Mukhopadhyaya, A. Nyffeler, Phys. Lett. B **649**, 280 (2007).
- [12] F. del Aguila, J. I. Illana, M. D. Jenkins, arXiv:0811.2891.
- [13] T. Han *et al.*, Phys. Rev. D **67**, 095004 (2003).
- [14] J. Hubisz, P. Meade, A. Noble and M. Perelstein, JHEP **01**, 135 (2006).
- [15] A. Djouadi, J. Kalinowski, M. Spira, Computl. Phys. Commun. **108**, 56 (2006).
- [16] See for instance: M. Spira, Fortsch. Phys. **46**, 203 (1998).
- [17] T. Han *et al.*, Phys. Lett. B **563**, 191 (2003).
- [18] R. Goncalo, arXiv:0811.3778.
- [19] D. Zeppenfeld *et al.*, Phys. Rev. D **62**, 013009 (2000).
- [20] J. Pumplin *et al.*, JHEP **0602**, 032 (2006).